Journal of Human Evolution 57 (2009) 63–74

Contents lists available at ScienceDirect

Journal of Human Evolution

journal homepage: www.elsevier.com/locate/jhevol

# Initial excavation and dating of Ngalue Cave: A Middle Stone Age site along the Niassa Rift, Mozambique

Julio Mercader [a,*], Yemane Asmerom [b], Tim Bennett [a], Mussa Raja [c], Anne Skinner [d]

[a] Department of Archaeology, University of Calgary, Alberta, T2N 1N4, Canada
[b] Department of Earth & Planetary Sciences, University of New Mexico, 200 Yale Blvd., NE, Albuquerque, NM 87131, USA
[c] Department of Anthropology and Archaeology, Universidade Eduardo Mondlane, Maputo, Mozambique
[d] Department of Chemistry, Williams College, 47 Lab Campus Drive, Williamstown, MA 01267, USA

ARTICLE INFO

*Article history:*
Received 24 September 2008
Accepted 22 March 2009

*Keywords:*
Southern Africa
Central Africa
Niassa Rift
Mozambique
Ngalue Cave
Electron Spin Resonance
U-series dating
Late Pleistocene
Middle Stone Age
Lithic analysis
Discoidal technology

ABSTRACT

Direct evidence for a systematic occupation of the African tropics during the early late Pleistocene is lacking. Here, we report a record of human occupation between 105–42 ka, based on results from a radiometrically-dated cave section from the Mozambican segment of the Niassa (Malawi/Nyasa) Rift called Ngalue. The sedimentary sequence from bottom to top has five units. We concentrate on the so-called "Middle Beds," which contain a Middle Stone Age industry characterized by the use of the discoidal reduction technique. A significant typological feature is the presence of formal types such as points, scrapers, awls, and microliths. Special objects consist of grinders/core-axes covered by ochre. Ngalue is one of the few directly-dated Pleistocene sites located along the biogeographical corridor for modern human dispersals that links east, central, and southern Africa, and, with further study, may shed new light on hominin cave habitats during the late Pleistocene.



## Introduction

Little is known about the demographics, behavioral profile, and ecological adaptability of the Middle Stone Age cultures that anteceded the Out-of-Africa migration (Mellars, 2006; Behar et al., 2008). The hypothesis that Pleistocene aridity fragmented tropical biomes and drove their inhabitants to isolated pockets that became havens from extinction has gained momentum in the light of new paleolimnological (Scholz et al., 2007; Cohen et al., 2007) and biomolecular (Manica et al., 2007) data from tropical Africa. These data depict eco-demographic scenarios in which megadroughts put Middle Stone Age populations under extinction stress. However, there is scant evidence for human occupation along the Western branch of the Great African Rift that presumably was roughly contemporaneous with these alleged climatic events, and this scarcity of evidence makes hypotheses about Middle Stone Age bottlenecks, refugia, and migration paths difficult to test in this region. Here, we provide an initial report on a Middle Stone Age site in a karstic setting located in the Mozambican segment of the Niassa (Malawi/Nyasa) Rift called Ngalue, and present for the first time the cave's archaeology, stratigraphy, and initial dating by Uranium-series, Electron Spin Resonance, and $^{14}C$. In this paper, we pay special attention to the techno-typological characterization of the Ngalue lithic assemblage and try to emphasize the importance of dating such stone repertoires for the study of the Middle Stone Age in this part of Africa.

The Lake Niassa region (also known as Malawi/Nyasa) has long been recognized as a steppingstone for the movement of people along the Great African Rift (Dixey, 1927; Clark, 1966; Juwayeyi and Betzler, 1995; Ring and Betzler, 1995; Betzler and Ring, 1995; Bromage et al., 1995). Yet, the Middle Stone Age of northern Mozambique remains almost completely unknown. Scientific investigations pertaining to early periods of biological and cultural evolution have not been conducted in Mozambique because of its remoteness, thirty years of war, and the slow, subsequent process of demining. Our work on the Mozambican Stone Age started in 2003 and it has few precedents. Previous work is limited to preliminary surface surveys and excavations (Borges, 1944; Simões, 1951, 1958; Barradas, 1962; Meneses, 1988, 1992; Sinclair et al., 1993) carried out south of the Limpopo, >1500 km south of our research area. Our focus is on the east-central segment of the Niassa Rift located

* Corresponding author.
*E-mail address:* mercader@ucalgary.ca (J. Mercader).

0047-2484/$ – see front matter © 2009 Elsevier Ltd. All rights reserved.
doi:10.1016/j.jhevol.2009.03.005

around Metangula (Fig. 1). The research area was chosen because of its proximity to: 1) the putative cradle for the origin of modern humans (Gonder et al., 2007); 2) the proposed population refugia at times of demographic bottlenecks and trans-African dispersals (Lahr and Foley, 1998); and 3) the wealth of archaeological sites uncovered through our survey (2003–2008) including deep, stratified cave deposits with well preserved, datable materials in the form of speleothems, tooth enamel, bones, and charcoal. Large-scale regional paleoclimatic data for the last 135 k. yr. are also available from the Lake Malawi drill sites located 100 km away (Scholz et al., 2007; Cohen et al., 2007; for a macro-regional view of ancient climates see the desiccation profile of Lake Victoria in Johnson et al. [1996]).

## Local geology and cave sedimentology

The Ngalue Massif is surrounded by four mountain ranges: Geci (North), Moombela (South), Chipilua (East), and Dilombe (West). These ranges represent some of the higher elevations in Mozambique, and are part of the crystalline basement composed of granodiorite, granosyenite, and granites formed in the Pan African Neoproterozoic (1000 Ma) (Lächelt, 2004). During the late Proterozoic (600 Ma), the basement was capped by crystalline limestones. These younger carbonate deposits are known in the geological cartography of Mozambique as the "Malulu" deposits (Lächelt, 2004), and their variable MgO contents and metaphormic grades determine the high variability in limestone types observed in the study area from pure limestones to dolomites and marbles. The Malulu deposits emerge from the adjacent landscape in distinctly pyramidal massifs that border the surrounding valleys of the Nankambe, Dikuyu, and Chitete Rivers that flow NE/SW into the Nnodwesi's watershed. One of these pyramidal limestone massifs, Ngalue, is the subject of on-going geoarchaeological research. This massif supports a main cave on a steep rocky slope 14 m above the present-day valley floor of the Chitete River, a small cavern on a smooth sedimentary slope several meters away from the Chitete, and several vertical shafts. Here, we report archaeological finds and geochronometric results from the main cavity (S 12°51.517'/E 35°11.902') (Fig. 2), which developed in a dark grey dolomitic marble. This dolomite has been subject to dissolution following a joint $\geq 60^{\circ}$ that governs water seepage and speleothem formation, mostly along the southern wall. Thin sections from cave wall samples (Buehler system: Petrothin; Isomet 4000; Metaserv 2000) and petrographic observation under the microscope (Olympus BX51) show that Ngalue's limestone is granoblastic, medium-to-coarse grained, and supports a uniform mosaic of sub-rhombohedral grains (for a survey of geoarchaeology and stratigraphic concepts in dolomite caves see Laville et al., 1980; Kuman and Clarke, 2000; Woodward and Bailey, 2000; Brain, 2004; Goldberg and Sherwood, 2006; Pickering et al., 2007).

The sedimentary sequence (Figs. 3 and 4) from bottom to top has five units. The bottom of the column is represented by the

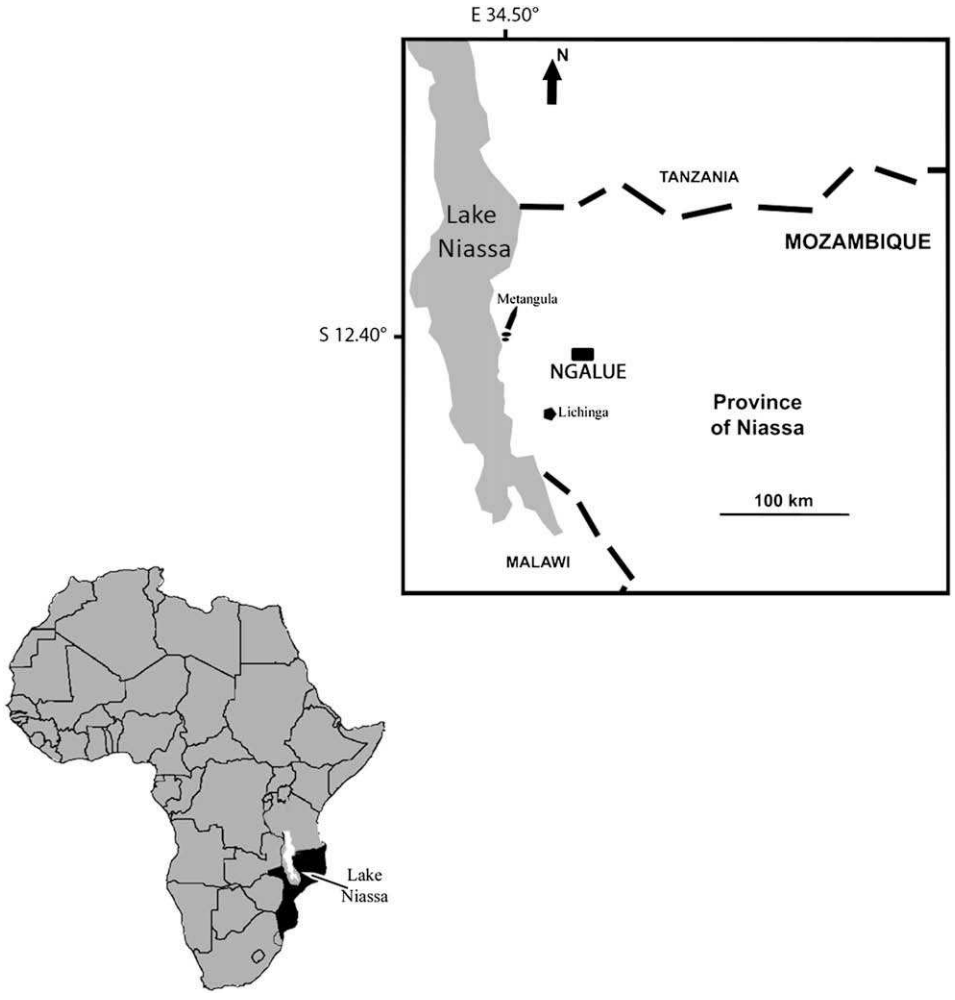


**Figure 1.** Study area and location of Ngalue cave in the Niassa Rift region.

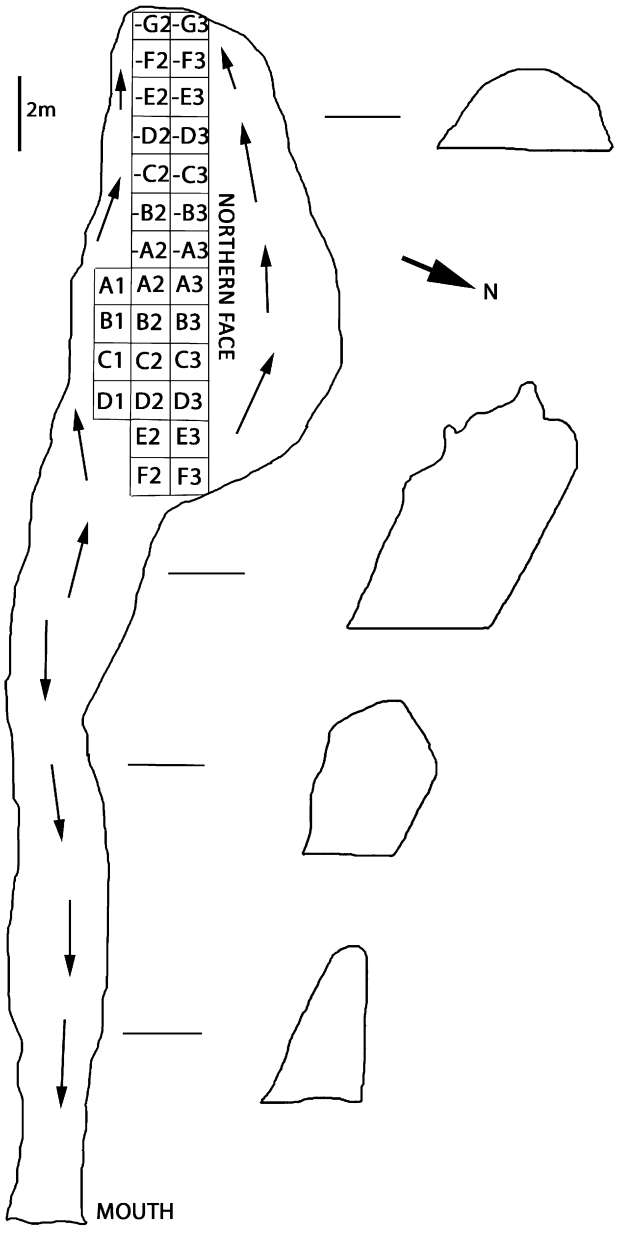


**Figure 2.** Map of Ngalue cave, cross sections of chambers, location of excavation grid, and position of the "Northern Face." Arrows indicate slope direction.

bare dolomite cave floor, which received speleothem and clastic facies. The earliest speleothem has a massive fabric, and it was secreted during the Middle Pleistocene (MIS 11/12: U-series age of 470 ± 48 ka; see Table 1 for all U-series ages). The clastic facies comprises alluvial sediments that entered the karst through the main mouth and were deposited in channels (troughs with upward fining pebbles and gravels) and low energy ponds (weakly bedded sandy silts with intercalated laminations of precipitated calcite). For this paleo-stream to enter the cave, we must assume a surrounding valley floor at least 15 m higher than it is today. Maximum thickness of the clastic facies is 0.8 m. Excavation did not retrieve stone tools or bone from the Basal Beds.

The Lower Beds were deposited between MIS 11 and MIS 5. Because of the large interval of geologic time that is not represented in this part of the column, we used a major hiatus to separate Lower Bed 1 from the overlying Lower Bed 2. Early on, the deepest sectors of the cave received a large volume of soft sediments (Lower Bed 1) that was covered by a (currently hanging) stalactite during MIS 8 (U-series age of 251 ± 51 ka). The base of this speleothem signals the existence of a cave paleo-floor 0.8 m higher than the modern floor (Figs. 3 and 4). Little has been preserved from this ancient body of sediments that existed under the stalactite due to erosion and subsequent transportation, presumably, elsewhere down the karst. Lower Bed 2 was deposited before the formation of a stalagmitic conglomerate (dated by U-series to 105 ± 13 ka) that caps the Lower Beds and separates, unconformably, Lower Bed 2 from the overlying Middle Beds. Lower Bed 2 also indirectly records speleothem activity in the cave in the form of boulder-sized stalactitic fragments that, although presently buried in Lower Bed 2, were portions of a hanging speleothem formed during MIS 9 (U-series age of 324 ± 14 ka). From a sedimentological perspective, the Lower Beds consist of poorly layered matrices enclosing moderately inclined flat slabs and pebble/cobble-sized cave spalls (a review of cryogenic debris deposits in Southern Africa can be found in Boelhouwers and Meiklejohn [2002]). Estimated thickness of the clastic sediments is 1.8 m. Lower Bed 2 contains fossil bone, teeth, and stone tools.

The archaeological horizons that are the focus of this article appear throughout the so-called Middle Beds and, in part, in Lower Bed 2. The body of sediments that make the Middle Beds in the main living area is wedge-shaped with a northern fill >1 m thick and a distal edge near the south end <0.5 m thick. The difference in deposit thickness indicates a sediment source entering the cave via an ancient chimney located in the northern segment of the main chamber's ceiling. The Middle Beds are spelothem-bound and consist of light, yellowish brown sediments rich in angular cave spall, lithics, animal bones, and teeth. Underneath, there is a stalagmitic conglomerate dated to 105 ± 13 ka. Above, there is a laminated flowstone dated by U-series to MIS 4 (55 ± 5 ka; 55 ± 14 ka). The age of the Middle Beds' upper boundary, ~50 ka, is confirmed by two congruent ESR dates from the base of the overlying Hearth Beds (see below, and Table 2).

The next stratigraphic unit exposed by our excavation is the Hearth Beds. These are matrix-supported, very pale brown sandy silts with fine unmistakable laminations, bedded structures, and interspersed guano horizons that comprise scarce cave spall, gravel, pebbles, and cobbles. Thickness is about 0.8 m. These beds contain stacked hearths, lithics, and faunal remains. ESR dating of two large mammalian teeth from the base of this unit yield two dates in agreement that indicate deposition ~50 ka (Table 2). Charcoal from a closed-context (hearth) dates the top part of these beds to AMS $^{14}$C >42 ka (Table 3).

Lastly, the most recent sedimentation is typified by the Capping Beds: ceramic/iron-bearing deposits dated by AMS $^{14}$C to Cal. AD 900-1040 (Table 3).

From a site formation point of view, the archaeological resolution available for Ngalue's Middle Beds is that of time-averaged palimpsests, as made clear by several observations including: 1) the complex polygenic nature of cave deposits, 2) the alternation of clastic and speleothem facies in the face of shifting climates and sedimentary cycles, 3) the existence of pronounced sedimentary gaps several times during the history of the cavity, 4) the sporadic nature of human occupation, and 5) the small sediment buildup that this cave recorded over a very long period of time. Horizontally, the highest concentration of materials takes place in the western grids (Fig. 5), which fits with the slope of the cave and may reflect gravitational and cultural displacement of debris towards the rear of the cave and lower surfaces.

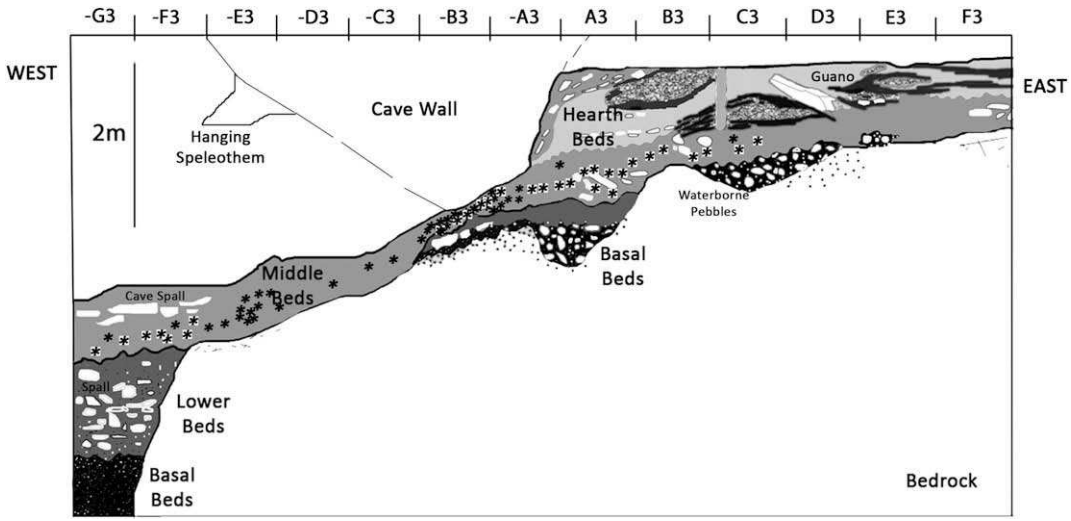


**Figure 3.** Stratigraphic section through the Northern Face. Asterisks indicate the Middle Beds' lithics from this part of the excavation.

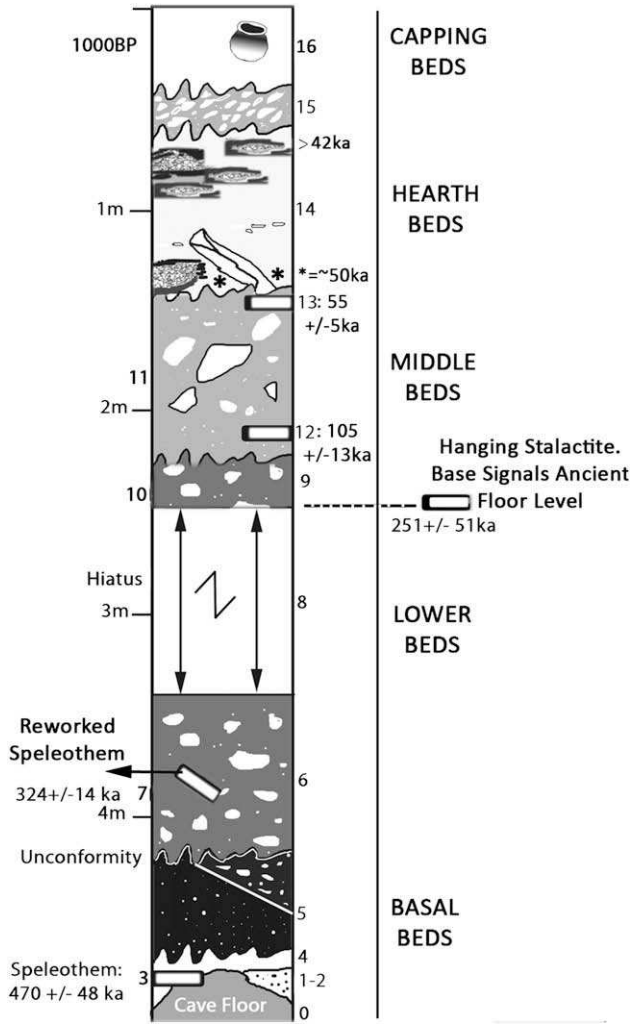


**Figure 4.** Idealized, composite stratotype from Ngalue Cave. Arabic numerals on both sides are the numbers assigned to a specific stratigraphic unit during excavation. Rectangles show the location of speleothems through the sequence.

## Excavation and lithics from the Middle Beds

The cave's longitudinal axis is aligned east to west (Fig. 2), with a mouth oriented 60° NE and a 20 m long corridor leading into a main chamber with a floor area of >50 $m^2$ and a ceiling height of ~8 m. Our trench exposed a 13 m long stratigraphic section ("Northern Face") that runs east/west and ends at the backwall (Figs. 2 and 3). The modern surface dips toward the east along the main corridor and deep inside to the west. Because cave sediments often display drastic lateral changes, JM excavated an alpha-numerical grid through 13 contiguous $m^2$, and each one of them was subdivided for excavation in 16 units measuring 25 cm by 25 cm. As a result, any artifact that was recovered at the sieve, as opposed to *in situ*, has a horizontal relocation error <12.5 cm. Further details on this type of excavation methodology can be found in Mercader et al. (2002). The calcareous sediment that covered artifacts made detection challenging and breathing hazardous. Trowels and brushes were used in the excavation of 5 cm artificial levels and natural layers. Sieving took place outside the cave through 1.8 mm wet sieves. Column sediments are very homogenous from a mineralogical perspective: oxides from calcium, phosphorus, and sodium as well as carbon dioxide (XRD: Electron Microbeam: JEOL JXA-8200; 5 WDS). Alkalinity is the norm (7.7–8.45; pH meter: Orion 310; by adding 7 ml of distilled water to 1 g of matrix, and vortexing prior to measurement in a 15 ml centrifuge vial). Organic matter content is low (<0.5% organic matter; 1.87 at 375 °C; loss on ignition; McKeague, 1976). Particle size analysis of the <2 mm fraction (analyzed using a "Malvern Mastersizer 2000" [Sperazza et al., 2004]) indicates a very similar matrix for all sediments, with a sandy silt texture in which sands amount to 18–43%. The mean particle size ranges from 12.7 μm–40.1 μm.

The total number of positively identified stone artifacts from the excavation of Ngalue cave during the 2007 season is 727. Three quarters of the total assemblage ($n = 555$) were found in the Middle Beds (Table 4). The archaeological influx of lithics into the Middle Beds' sediments over time (Fig. 6) was low and reflects a fluctuating nature. These small numbers per spit advise against undertaking detailed quantification of artifact densities and types level by level. Our lithic descriptions, therefore, apply to the entire collection from the Middle Beds. It is important to note that faunal, paleobotanical, geoarchaeological, and chronometric analyses are still on-going, and further details will be published elsewhere in the near future.

**Table 1**
Uranium-series data for Ngalue speleothems.

| Sample | U (ppb) | Th (ppb) | $^{230}Th/^{238}U$ (activity) | * $\delta^{234}U$ (measured) | $\delta^{234}U$ (initial) | Age (ka) (uncorrected) | Age (ka) (corrected) |
|---|---|---|---|---|---|---|---|
| NGA-A | 917.2 ± 2.4 | 459 ± 1 | 0.584 ± 0.003 | 253 ± 2 | 295 ± 6 | 66.86 ± 0.45 | 55.06 ± 5.77 |
| NGA-B | 333.8 ± 1.0 | 392 ± 1 | 0.676 ± 0.004 | 212 ± 2 | 248 ± 11 | 86.43 ± 0.74 | 55.20 ± 14.58 |
| NGA-C | 91.7 ± 0.2 | 3.88 ± 0.05 | 1.137 ± 0.008 | 149 ± 2 | 371 ± 16 | 325.10 ± 14.3 | 324.20 ± 14.17 |
| NGA-E | 129.1 ± 0.4 | 2.43 ± 0.05 | 1.193 ± 0.006 | 254 ± 3 | 517 ± 10 | 251.43 ± 5.17 | 251.07 ± 5.16 |
| NGA-F | 890.7 ± 2.4 | 970 ± 3 | 0.855 ± 0.004 | 178 ± 3 | 239 ± 10 | 134.2 ± 1.35 | 105.33 ± 13.58 |
| NGA-I | 201.9 ± 0.7 | 0.1 ± 0.1 | 1.221 ± 0.007 | 171 ± 3 | 645 ± 95 | 470.47 ± 48.27 | 470.46 + 48.27 −37.14 |

Corrected ages use an initial $^{230}Th/^{232}Th$ atomic ratio = 4.4 ± 2.2 ppm. All errors are absolute 2σ. Subsample sizes range from 85 mg to 105 mg.
* $\delta^{234}U$ = the permil variation of the measured $^{234}U/^{238}U$ atomic ratio from the secular equilibrium ratio, which is equal to $\lambda_{238}/\lambda_{234}$.
$\lambda_{230} = 9.1577 \times 10^{-6}\ y^{-1}$, $\lambda_{234} = 2.8263 \times 10^{-6}\ y^{-1}$, $\lambda_{238} = 1.55125 \times 10^{-10}\ y^{-1}$ (Cheng et al., 2000).

The main raw material employed for lithic production was local quartz from cobbles and rock veins. Because pegmatite and quartzitic dykes are not part of the natural configuration of the Ngalue massif or cave, nor are alluvial sediments part of the Middle Beds, all artifacts unearthed in the Middle Beds have been interpreted as being brought into the cave by human action, after which they may have been subjected to short distance transport within the cavity by natural and anthropogenic forces. Artifacts are in fresh condition. Because clast rounding and fluvial sedimentological structures are both absent from the Middle Beds, we infer minimal water disturbance to the lithic assemblage. The petrographic nature, grain, and conchoidal properties of the raw materials used for lithics are variable, and therefore we should refrain from imposing preconceived technical limitations to stone knapping derived from the raw material alone. Stereotypes typically portray quartz as a last-resort material, lacking technological and typological signatures, and with internal crystalline flaws that predetermine the final (fortuitous) shape of the blank as well as its small size. Yet, Middle and Later Stone Age assemblages from the African woodlands and rainforests show that quartz can be a deliberate choice even in places where other raw materials are available (Mercader and Martí, 2003). It can also yield reasonably large instruments (Mercader and Martí, 2003; Mercader et al., 2008: Fig. 3), as well as microliths (Mercader, 2003). Quartz supports both expedient and standardized reduction sequences. These sequences do leave material signatures on flakes and cores (Mercader and Brooks, 2001) and these sequences have been published by prominent research groups in adjacent countries such as Malawi (Mwanganda: Clark and Haynes, 1970) and Zambia (Twin Rivers: Barham, 2000; Clark and Brown, 2001; Mumbwa: Barham, 2000). We have no doubt that the application of specific technological schemes to quartz reduction produces consistent lithic morphotypes, but the rigid physical properties and internal flaws that some quartz specimens possess introduces a degree of unpredictable intra-type variability that makes typological classification challenging. Yet, reduction schemes and consistent tool types can be identified (Table 5). The five diagnostic features that define Ngalue's lithic assemblage from the Middle Beds are as follows: 1) nearly exclusive use of quartz, except for a few pieces of quartzite; 2) discoidal reduction, although simple reduction (*sensu* Mercader 2003) is present; 3) core size bimodality around the 40 mm boundary; 4) handheld, and, in the case of small cores, braced reduction (*sensu* Barham, 1987); and 5) levallois, bipolar technique, Modes 4–5, and systematic retouch are all minimal.

Overall, the idealized stone piece from Ngalue cave measures 50 mm in maximum length (range: 15–180 mm), and weighs 85 g (range: <1–1000 g). Reports from on-going morphometric and techno-typological analysis are forthcoming. Generally speaking, we can say that cores are very abundant, flakes are scarce, and formal tools are present. There are undetermined fragments, along with preparation products, rejuvenation pieces, and shatter. Although some microliths are present, Ngalue's lithics do not constitute a microlithic or blade assemblage from metric, technological, or compositional perspectives. From a quantitative standpoint, a subset of lithics from artifact-rich ($n = 281$, 50% of the entire Middle Beds' assemblage) and spatially discreet (1 $m^2$) grid –E2 illustrates the makeup of Ngalue's lithics in which cores represent one third of the entire assemblage. Here, at grid –E2, 80% of the cores are discoidal and the rest are simple platform types (Fig. 7). Discoidal cores may display preferential exploitation of one side (pseudo-Levallois 88%) or two opposing extraction volumes (12%) (Fig. 7). In spite of a clear dominance of cores with preferential exploitation of one side (pseudo-Levallois), the flakes that presumably came off this type of core are scarce (Fig. 8).

Size bimodality is clear for all core types (Fig. 7). For example, one third of the cores in the discoidal category are miniature discoidal cores of <40 mm in maximum length, while the remainders belong to larger size categories. Formal types or tools include pointed products (Fig. 8), scrapers (Fig. 9), awls (Fig. 8), and microliths (Fig. 8) (Table 5). Special objects (Fig. 10) include a rhyolite grinder/core-axe, a rhyolite ground cobble, and a faceted quartz core tool. The last two pieces were flaked on one side to create a dish, resembling "metates" or passive grinding stones. All three appear covered with red or orange pigments, and in one case the patina over the ochre suggests an exposure to silica-rich plant tissue.

**Table 2**
Electron Spin Resonance data for Ngalue teeth (Hearth Beds).

| Sample data | | [U]ppm | AD (Gy) | $D_{int}$ (mGy/a) | $D_{ext}$ (mGy/a) | EU Age (ka) | LU Age (ka) |
|---|---|---|---|---|---|---|---|
| PT21/Nga, 8; Grid A3, Spit 9, Square 5, △ 0.6 m | Enamel, 1 | 0.03 ± 002 | 42.27 ± 2.11 | 0.041 ± 0.004 | 0.894 ± 0.06 | 43.11 ± 3.56 | 45.25 ± 3.72 |
| | Enamel, 2 | | 38 ± 1.76 | 0.044 ± 0.003 | 0.894 ± 0.06 | 38.8 ± 3 | 40.64 ± 3.25 |
| | Dentine, 1 | 2.03 ± 0.02 | | | | | |
| | Dentine, 2 | 1.75 ± 0.02 | | | | | |
| PT23/Nga, 10; Grid B3, Spit 9, Square 7, △ 0.6 m | Enamel, 1 | 0.03 ± 002 | 48.98 ± 2.86 | 0.091 ± 0.005 | 0.886 ± 0.06 | 46.2 ± 3.83 | 50.66 ± 4.35 |
| | Enamel, 2 | | 48.63 ± 2.94 | 0.081 ± 0.005 | 0.886 ± 0.06 | 45.98 ± 3.87 | 50.32 ± 4.4 |
| | Cementum | 4.38 ± 0.02 | | | | | |
| | Dentine, 1 | 4.72 ± 0.02 | | | | | |
| | Dentine, 2 | 3.72 ± 0.02 | | | | | |

**Table 3**
AMS $^{14}C$ data for Ngalue samples from Hearth and Capping Beds.

| Sample data | Material | Stratigraphic unit | Radiocarbon age BP | $^{13}C/^{12}C‰$ |
|---|---|---|---|---|
| Beta-235578 | Charred Remains | Capping Beds | 1030 ± 40 | −24.5 |
| Beta-236941 | Organic Material | Hearth Beds | 43120 ± 920 | −25.1 |

Techno-typologically, the assemblages from the Middle Beds resemble those from other Middle Stone Age sites located in Malawi, Tanzania, Zambia, and Zimbabwe (Armstrong, 1931; Clark and Haynes, 1970; Barham, 2000; Clark and Brown, 2001; Willoughby, 2001). A comparative, semi-quantitative analysis of Ngalue's techno-typological features with selected sites from these countries (Table 5) indicates that the closest affinity with the Mozambican lithics is in Kalambo Falls and Twin Rivers, followed by Mumbwa, and to a lesser extent by Mwanganda and the Songwe Basin sites. However, because of the unpublished or qualitative nature of pertinent finds from Malawi and southern Tanzania, the behavioral meaning of these gross affinities remains unclear.

## Geo-chronometry

### *Uranium-series dating*

The uranium-series method of dating is based on the decay of $^{234}U$ to $^{230}Th$. An ideal material for dating using this method is one that incorporates uranium but excludes thorium in its crystal structure. Cave speleothems are thus excellent materials for U-series dating because speleothem calcite typically contains high U/Th ratios and are preserved well in cave environments. For older samples, it is possible to get reliable absolute ages even in cases where the U/Th is not high because the small amount of unsupported $^{230}Th$, which is a few parts per million of the common thorium, becomes a small fraction of the total $^{230}Th$.

The U-series isotope measurements were conducted at the Radiogenic Isotope Laboratory, University of New Mexico. Clean carbonate was drilled and dissolved in nitric acid and spiked with a mixed $^{229}Th$-$^{233}U$-$^{236}U$ spike. U and Th were separated using conventional anion exchange chromatography. Most of the U and Th measurements were done on a Neptune multi-collector inductively coupled plasma mass spectrometer (MC ICP-MS). In the MC ICP-MS, all U and Th isotopes were measured in a static mode utilizing a mix of $10^{11}$ and $10^{12}$ ohm resistors and an ion-counting SEM (Asmerom et al., 2006). SEM-Faraday gain was established using a CRM-145 U standard for U and an in-house Th standard for Th analyses. Mass fractionation correction was done using the $^{233}U/^{236}U$ ratio of 1.0046 for U isotope analyses. For Th analyses, standard-sample bracketing was used to correct for mass fractionation and instrument drift. CRM-145 U isotope standard was measured with the samples obtaining the conventionally accepted $\delta^{234}U$ value of $-36.5 \pm 0.5‰$ [S2]. $^{234}U = [[^{234}U/^{238}U_{\text{sample}}/^{234}U/^{238}U_{\text{secular equilibrium}}]-1] \times 10^3$, where, $^{234}U/^{238}U_{\text{secular equilibrium}} = \lambda_{238}/\lambda_{234}$. U and Th procedural blanks were 5–10 picograms and therefore have no effect on the ages. The age uncertainties include analytical errors and uncertainties in the initial $^{230}Th/^{232}Th$ ratios.

Our analysis returns a series of dates ranging from 105 ± 13 ka to 55 ± 5 ka (Table 1). The age uncertainties only reflect analytical errors. The combined external analytical errors are better than 1%. The second group of ages (last column of Table 1) reflect uncertainties due to initial $^{230}Th$ correction, assuming a typical crustal Th/U ratio of 3.8, which translates to a $^{230}Th/^{232}Th$ ratio of $4.4 \times 10^{-6}$. The approach to the initial Th correction is validated by the age data from samples Ngalue-A and Ngalue-B. These are samples from the same horizon. Although they have large

**Table 4**
Vertical distribution of lithics per excavation zone.

| Grids | Hearth Beds | Middle Beds | Lower Beds |
|---|---|---|---|
| F2-F3 | 3 | 0 | 0 |
| E2-E3 | 0 | 0 | 0 |
| D1-D2-D3 | 0 | 3 | 0 |
| C1-C2-C3 | 13 | 22 | 0 |
| A1-A2-A3 | 6 | 46 | 0 |
| B1-B2-B3 | 5 | 17 | 0 |
| (-)A2/A3 | 0 | 26 | 0 |
| (-)B2/B3 | 0 | 74 | 0 |
| (-)C2/C3 | 0 | 7 | 0 |
| (-)D2/D3 | 0 | 1 | 0 |
| (-)E2/E3 | 0 | 227 | 82 |
| (-)F2/F3 | 0 | 27 | 13 |
| (-)G2/G3 | 0 | 105 | 50 |
| Subtotals | 27 | 555 | 145 |

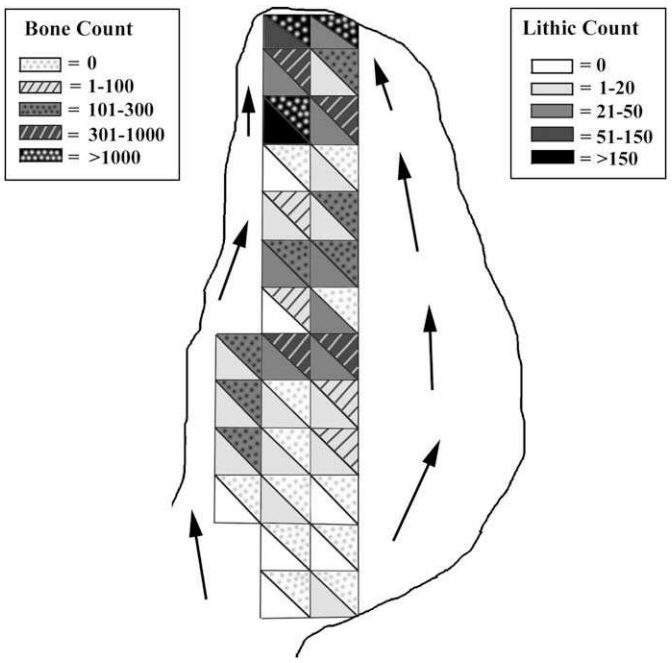


**Figure 5.** Spatial distribution of lithics and bones at Ngalue cave. Designed by K. Griffith.

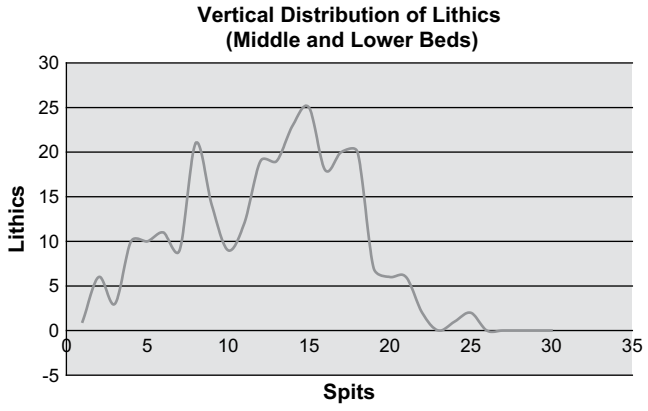


**Figure 6.** Nature and rate of lithic influx into the Middle and Lower Beds as seen in grid -E2.

**Table 5**
Techno-typological description of formal tools.

| Tools | Mwanganda[a] | Kalambo Falls[b] | Mumbwa[c] | Twin Rivers[d] | Songwe Basin[e] |
|---|---|---|---|---|---|
| Discoidal core (preferential) | X | X | X | X | |
| Discoidal core (opposing extraction volumes) | X | X | X | X | |
| Miniature discoidal core | X | X | X | X | X |
| Simple reduction (multiple platforms) | | X | X | X | |
| Tool type 1a | | X | | | |
| Tool type 1b | | X | | | |
| Tool type 1c | | | | X | |
| Tool type 2a | | X | | X | |
| Tool type 2b | X | X | | | |
| Tool type 2c | X | X | X | X | |
| Tool type 2d | X | X | | | |
| Tool type 3a | | X | X | X | |
| Tool type 3b | | | | X | X |
| Tool type 4a | | | X | X | X |
| Tool type 4b | | | X | X | X |
| Core-Axe | | X | | X | |

**X** = documented
blank = undocumented/unclear

Tool type no. 1: Point
1.a. Levallois-like ($n = 1$) (Fig. 8a).
1.b. Flake struck from a discoidal core with a resulting kite morphology, in which one side is formed by the platform ($n = 1$) (Fig. 8b).
1.c. Acute-angled piece with a triangular cross section and distinctly steep angles that range from 25–50°. (The ventral surface is a rejuvenated platform produced by striking the ridge of a core). Some specimens display shoulder and tang ($n = 6$) (Fig. 8k, l).
Tool type no. 2: Scraper
2.a Core-scraper (*sensu* Mercader and Brooks, 2001: 208). These are made on small core fragments or on exhausted cores. All of them have in common the steep scraping edge made by invasive peripheral retouch. They are distinguished from small cores by the creation of a flat base, small regularizing retouch, and/or utilization creating a smooth, rounded scraping or platform edge ($n = 11$) (Fig. 9a, b).
2.b Scraper on core fragment: slightly convex or nosed scraping edge created by peripheral retouch. Most examples ($n = 4$) have a flat rejuvenation base, except for one specimen ($n = 1$) (Fig. 9c).
2.c Side scraper on flake ($n = 1$) (Fig. 9e).
2.d Denticulate ($n = 1$) (Fig. 9d).
Tool type no. 3: Awl
3.a Drill tip formed by opposing removals ($n = 1$) (Fig. 8h).
3.b Drill tip formed by a double burin ($n = 2$) (Fig. 8g).
Tool type no. 4: Microlith
4.a Small thumbnail piece <20 mm. Circular radial flake with minute platform and scarce retouch ($n = 2$) (Fig. 8c, d).
4.b Crescent. Flake shaped to a lunette morphology ($n = 2$) (Fig. 8e, f).
[a] Clark and Haynes (1970).
[b] Clark (2001).
[c] Barham (2000).
[d] Barham (2000), Clark and Brown (2001).
[e] Willoughby (2001).

differences in U/Th ratios and apparent ages, their initial $^{230}Th/^{232}Th$ ratio corrected ages converge.

*Electron Spin Resonance dating*

Approaches such as "Trapped Charge Methods," (e.g., Electron Spin Resonance or ESR) can detect free radicals created when radiation breaks stable chemical bonds. The first systematic use of ESR for dating was the work of Ikeya (1975) on Japanese stalagmites. While other sources of calcium carbonate (coral reefs, shells, spring deposits) were initially the study materials, geologists have also studied quartz to investigate tectonic motion (e.g., Fukuchi, 2001), and ESR has been used to study heated flint (Skinner and Rudolph, 1997). Good general references have been written by Rink (1997) and Blackwell (2001). In recent years, attention has shifted to tooth enamel. Tooth enamel is the hardest tissue in the body, and therefore teeth are often preserved in sites that are otherwise barren of fossil remains. The ESR signal in enamel is remarkably stable (Skinner et al., 2000), so that, in theory, one can date teeth as young as a few thousand years old and as old as the Miocene. The limiting factor becomes saturation of radiation damage in the tooth enamel and not signal stability.

To date a material by ESR, one takes aliquots of a sample and irradiates them with known doses. Back extrapolation of dependence of signal intensity on dose (the "growth curve") allows one to determine the total dose experienced by the sample since its formation (the "accumulated dose"). To calculate the age of the sample one uses the following equation:

$$A_\Sigma = A_{int} + A_{ext} = \int_0^{t_1} D_\Sigma(t)dt = \int_0^{t_1} (D_{int}(t) + D_{ext}(t))dt$$

where $A_\Sigma$ = the total accumulated dose in the sample
$A_{int}$ = the internally derived accumulated dose component
$A_{ext}$ = the externally derived accumulated dose component
$D_\Sigma(t)$ = the total dose rate
$D_{int}(t)$ = the total dose rate from within the sample
$D_{ext}(t)$ = the total dose rate from the external environment
$t_1$ = the sample's age
$t$ = time

For teeth, the internally derived dose arises from uranium in the dentine and enamel. In order to find the external dose rate, soil

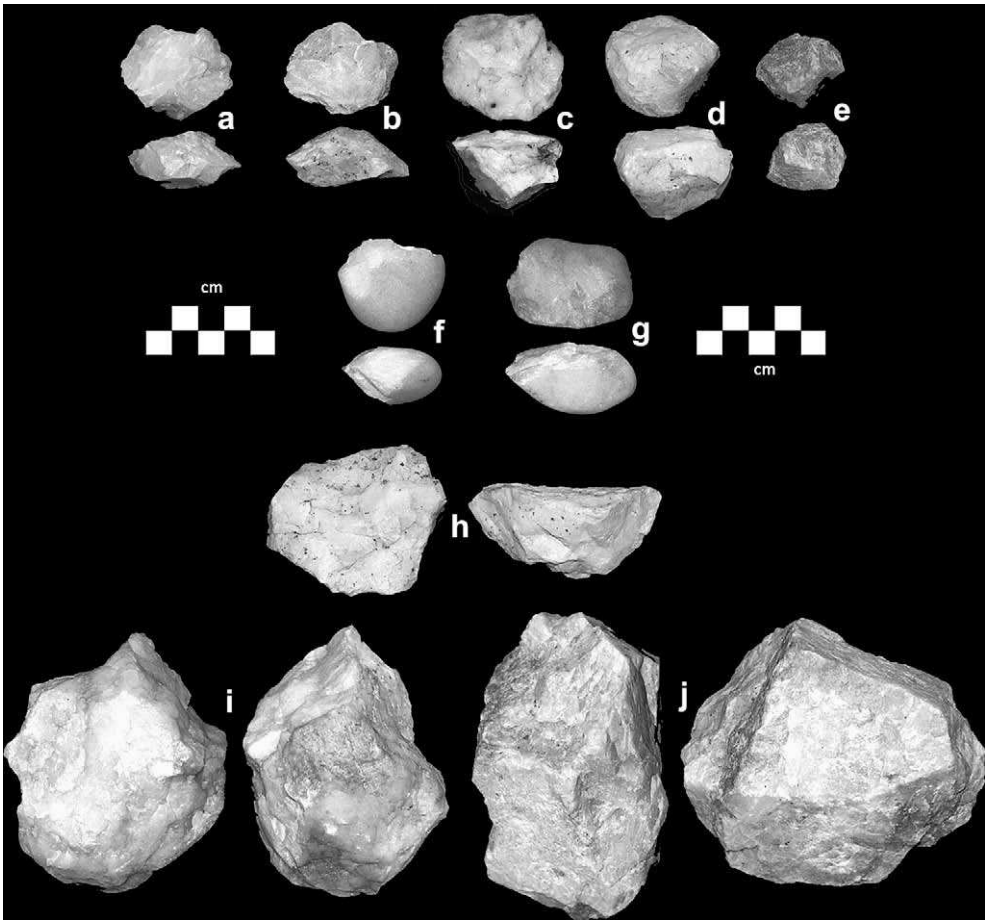


**Figure 7.** Core technology from Ngalue cave: a, b) discoidal, exploitation of both sides; c, d, e, h) discoidal, preferential exploitation of one side; f, g) cores on small river pebbles displaying incipient reduction or testing; i, j) simple platform cores (large size).

radioactivity, moisture, and possible cosmic radiation must be measured. The deficiencies of ESR arise primarily from its dependence on the environment. For example, if environmental radiation changes because of climatic change, the accumulation of radiation damage will not be a linear function of time. The environment also affects the internal dose rate, in that teeth are not closed systems. Both dentine and enamel can absorb uranium from ground water; thus, changes in U concentrations must also be modeled. Recently, coupling ESR with U/Th (also called "uranium series") dating has been successful in proving the appropriate model (e.g., Zhou et al., 1997). The U/Th method cannot give ages for open systems, but the uptake effect is opposite to that for ESR, and so by iterating the two apparent ages, a true age can be found.

Mammalian tooth samples from the Hearth Beds at Ngalue cave were prepared by standard techniques (Skinner et al., 2005). Dentine and enamel were separated by mechanical drilling and enamel powdered in an agate mortar to 38–90 μm. The teeth were sufficiently large that several subsamples could be obtained, with at least 13 aliquots each. Artificial irradiation to a maximum dose of 500 Gy (≥10 times the AD) used a $^{137}$Cs source with a dose rate of 238 rad/min. Measurements were made on a JEOL RE1X spectrometer at a power of 2 mW and modulation amplitude of 0.1 mT, at a scan rate of 12.5 mT/min. The dependence of signal intensity on dose plotted (growth curve) assumed a saturating exponential regression. Back extrapolation of the plot yielded the accumulated dose (AD) or the total amount of damage. The average annual dose rate the sample had experienced was found by neutron activation analysis (NAA) of dental tissues and surrounding sediment. As every sedimentary element within 30 cm of the sample contributes to the dose, we generally measured up to six sediment samples for each tooth, all taken within a 30 cm radius. While the radioisotope content of all sediments for PT21 and PT23, including those taken directly off the teeth, seemed quite uniform, we anticipate confirming this with additional sediment samples. Our ages have been calculated using the program ROSY (Brennan et al., 1997), which considers beta-attenuation in the tooth precisely. Although we report EU and LU ages, with the small amount of uranium in these enamels the calculated ages do not depend significantly on uptake model. The low uranium content detected in the samples also made it unlikely that coupled ESR/U series dates could be obtained. Other assumptions were: 1) sedimentary water content of ~15%, 2) no cosmic dose, and 3) use of standard parameters for the dosimetry in teeth. The present-day sedimentary water content is less than 15%, but processes of cave formation require that it be higher in the past. Our results yield a series of assays between 50 ± 4 ka and 40 ± 3 ka (Table 2).

### *AMS $^{14}$C dating*

The radiocarbon-dated material included charred and organic samples (all $^{14}$C dates are reported in Table 3). The youngest sample dates to the Late Iron Age occupation of the cavity, and it was found in association with ceramics and iron. The older sample comes from hearth number 3A (grid D3, absolute depth of 0.25 m), in the Hearth Beds, and the age reported was obtained on organic materials (43 ± 0.9 ka). For the latter assay, we note that the $^{14}$C

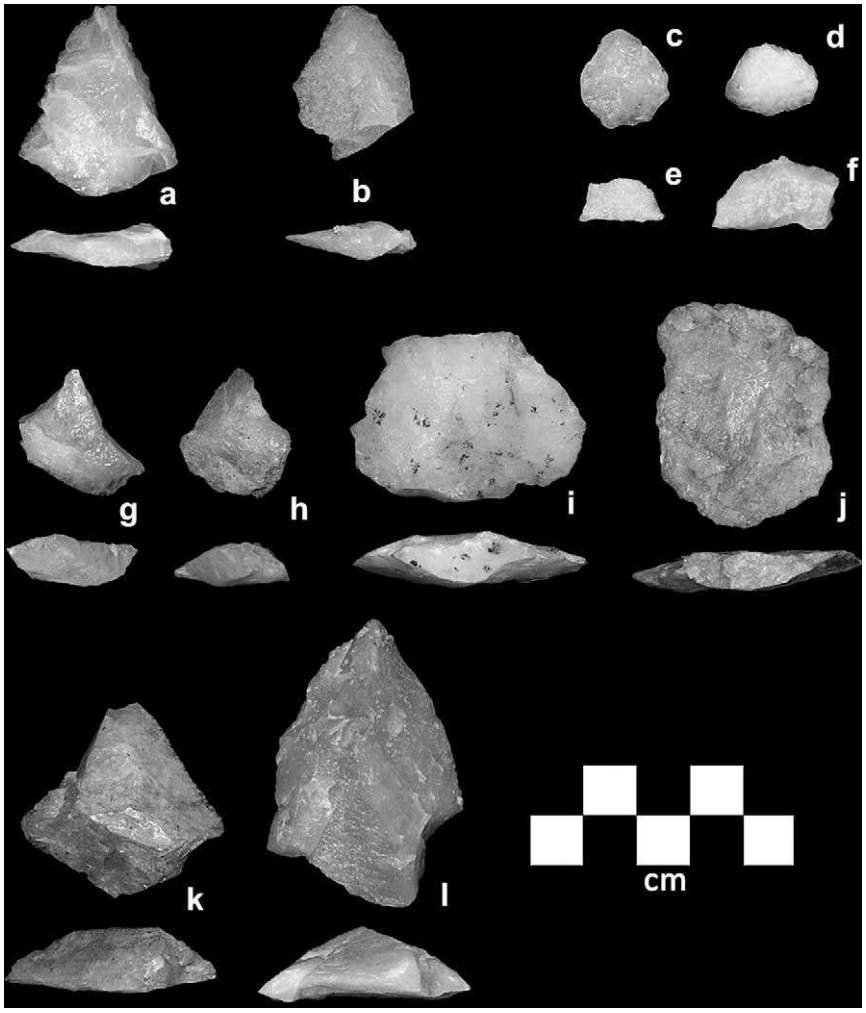


**Figure 8.** Points, awls, flakes, and microliths from Ngalue Cave: a) pseudo-Levallois point; b) pointed discoidal flake; c, d) microlithic thumbnail pieces; e, f) crescents; g) drill tip formed by double burin blows; h) awls formed by opposing removals; i, j) pseudo-Levallois flakes; k, l) pointed tools with incipient shoulders and tangs.

signature was found to be just outside statistical agreement with the background. Therefore, indeterminate error could swing this result to an infinite age. Conservatively, this result is best interpreted as >42 ka.

## Discussion and concluding remarks

We have provided the initial geoarchaeological context, absolute dating, and finds from a Middle Stone Age cave occupation that puts the Niassa Rift Region of Northern Mozambique on the map of modern human origins research for the first time and paves the way for future research into Mozambique's distant past. This is the first time that Middle Stone Age lithics from Northern Mozambique have been dated by absolute means. The interpretation of equatorial and southern hemisphere lacustrine data sets (Johnson et al., 1996; Scholz et al., 2007) indicates that climate fluctuated widely during the Middle and Late Pleistocene in the study area. Paleoanthropologists have frequently assumed that the higher rainfall region that currently supports woodlands along the Western Branch of the Great African Rift was more or less continuously inhabitable during these fluctuations (Lahr and Foley, 1998) at a time when severe aridity and dramatic mega-droughts rendered much of the continent uninhabitable (Marean and Assefa, 2005; Scholz et al., 2007). However, little direct evidence of human occupation dated to the early Late Pleistocene has been found yet in this part of Africa. Here we have shown, based on results from a radiometrically-dated cave section from the Mozambican segment of the Malawi (Nyasa/Niassa) Rift called Ngalue, a record of human occupation between 105–42 ka during the Middle Stone Age. Ngalue contains evidence of human presence in the cave during multiple inhabitation episodes of unknown duration each. These occupations were spread over the course of more than 50,000 years. They represent the only terrestrial record available for the reconstruction of human settlement on the Mozambican side of the central Malawi basin (cf. Clark and Haynes, 1970; Bromage et al., 1995; Juwayeyi and Betzler, 1995; Cohen et al., 2007; Scholz et al., 2007) and one of the few directly-dated Pleistocene sites located along the biogeographical corridor for modern human dispersals that links east, central, and southern Africa (cf. Barham, 2000).

In the future, the on-going search for paleo-vegetational and climatic clues in Ngalue's clastic, isotopic, and speleothem records will identify the paleo-environments that surrounded early *Homo sapiens* from the Niassa Rift and their change over time. These bases will allow us to depict the variability of local ancient landscapes and subsistence modes. They will provide a frame to test whether or not the behavioral signal from Middle Stone Age industries responds to specific ecological imprint (cf. Marlowe, 2005; McCall, 2007), and if environmental/paleo-habitat change over short time

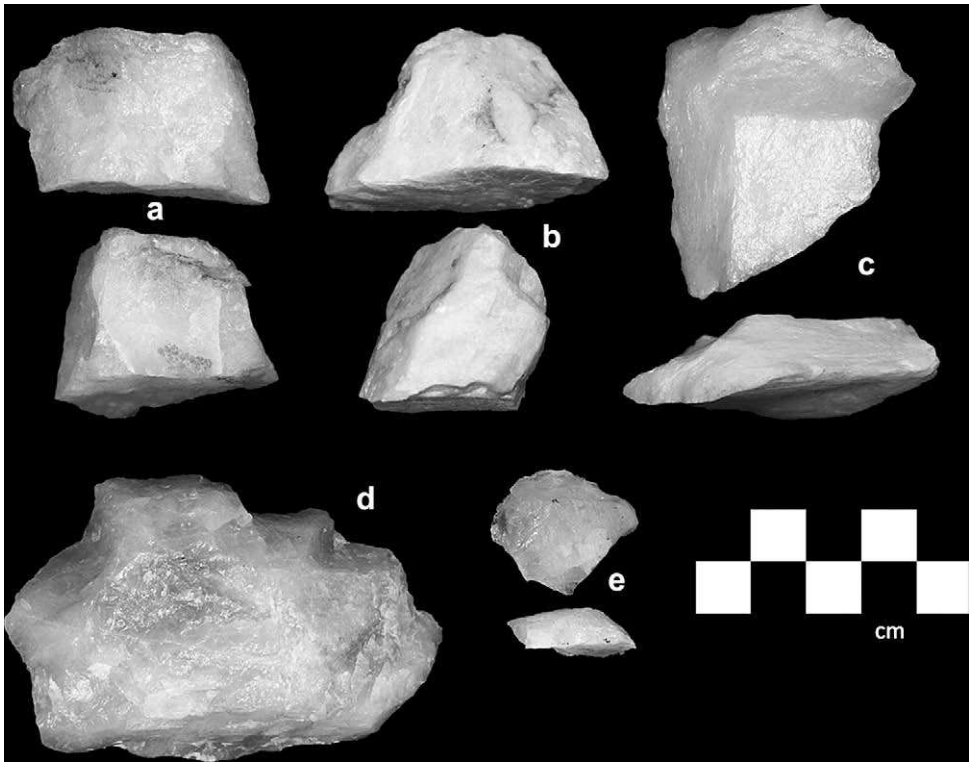


**Figure 9.** Scrapers: a, b) core-scrapers, c) scraper on core fragment, d) large denticulate, e) side scraper on flake.

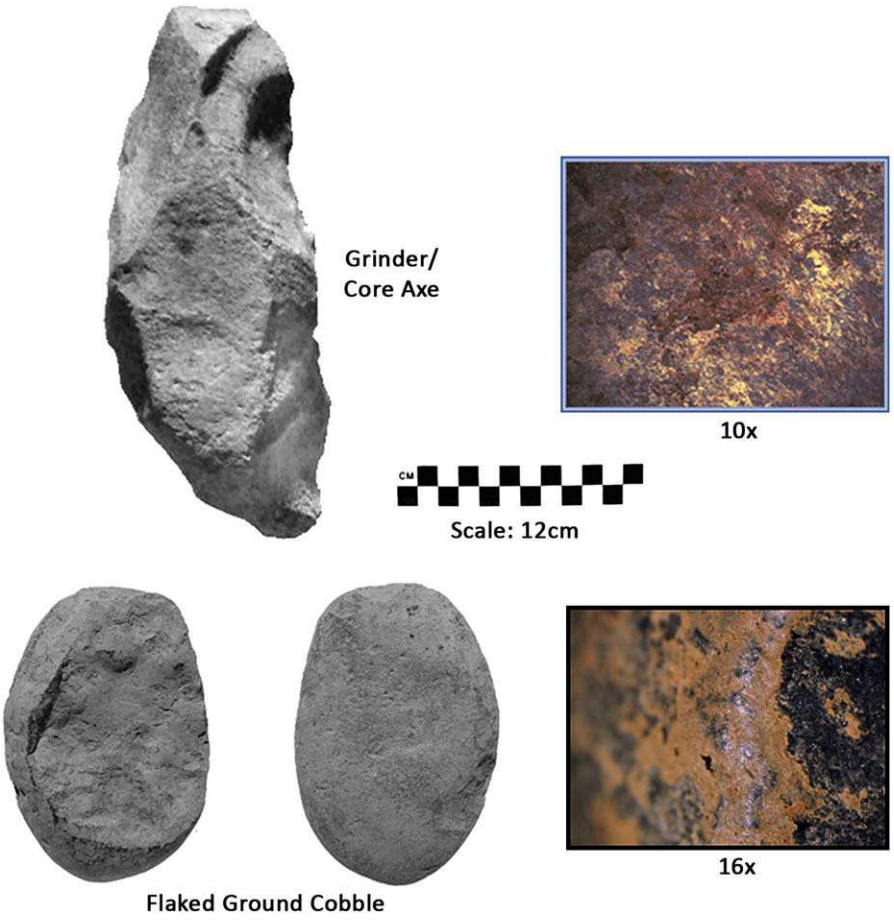


**Figure 10.** Grinders and ochre from the Middle Beds of Ngalue.

scales (Scholz et al., 2007; Cohen et al., 2007) determines inter-regional industrial variation (Clark, 1988; Barham, 2001) and human evolutionary ecology (Kingston, 2007).

## Acknowledgments

We thank Hilário Madiquida, Eduardo Mondlane University in Maputo and the Mozambican Ministry of Education and Culture (03-2003 and 01-2007). Temporary export of materials was conducted under "Certificate of Origin no. 0134" from the Mozambican Chamber of Commerce, as well as the "Export License no. 24399" from the Mozambican Customs Service. We thank the Canada Research Chairs program and the Canada Foundation for Innovation for making much of this research possible through generous grants and research endowments (CFI grant no. 201550) to the lead author and the Tropical Archaeology Laboratory at the University of Calgary. The Faculty of Social Sciences, the Dept. of Archaeology, and various internal programs at the University of Calgary made available financial and logistical support to JM. The Social Sciences and Humanities Research Council of Canada (File no. 410-2007-0697; CID: 148244), as well as the American Embassy in Maputo (Ambassador's Fund for Cultural Preservation) assisted this project with essential monetary aid. We thank National Geographic for their funding (NGS grant #8177-07). The Department of Anthropology at the George Washington University and the Human Origins Program at the Smithsonian Institution provided institutional support. We thank Williams College, Wadsworth Laboratories of the New York Department of Public Health. NAA analysis was performed at McMaster University Nuclear Reactor. Funding for ESR measurements came from NSF Grant ILI 9151111 and Williams College. Three anonymous referees provided rigorous peer review and improved our article significantly.

## References

Armstrong, A.L., 1931. Rhodesian archaeological expedition (1929): excavation in Bambata cave and researches on prehistoric sites in southern Rhodesia. J. Roy. Anthropol. Inst. Great Brit. Ireland 61, 239–276.

Asmerom, Y., Polyak, V., Schwieters, J., Bouman, C., 2006. Routine high-precision U–Th. isotope analyses for paleoclimate chronology. Geochim. Cosmochim. Acta 70, A24.

Barham, L., 1987. The bipolar technique in Southern Africa: a replication experiment. The South African Archaeological Bulletin 42, 45–50.

Barham, L., 2000. The Middle Stone Age of Zambia, South Central Africa. Western Academic and Specialist Press, Bristol.

Barham, L., 2001. Central Africa and the emergence of regional identity in the Middle Pleistocene. In: Barham, L., Robson-Brown, K. (Eds.), Human Roots: Africa and Asia in the Middle Pleistocene. Western Academic and Specialist Press, Bristol, pp. 65–80.

Barradas, L., O Quaternário do Antigo lago Lunho e da margem Portuguesa do lago Niassa. Direcção Nacional de Geologia, Maputo. (1962) (unpublished report).

Behar, D., Villems, R., Soodyall, H., Blue-Smith, J., Pereira, S., Metspalu, E., Scozzari, R., Makkan, H., Tzur, S., Comas, D., Bertranpetit, J., Quintana-Murci, L., Tyler-Smith, C., Wells, R., Rosset, S., 2008. The dawn of human matrilineal diversity. Am. J. Hum. Genet. 82, 1130–1140.

Blackwell, B.A.B., 2001. Electron Spin Resonance (ESR) dating in lacustrine environments. In: Last, W.M., Smol, J.P. (Eds.), Tracking Environmental Change Using Lake Sediments: Basin Analysis, Coring, and Chronological Techniques, 1. Kluwer, Dordecht, pp. 283–368.

Boelhouwers, J., Meiklejohn, K., 2002. Quaternary periglacial and glacial geomorphology of southern Africa: review and synthesis. S. Afr. J. Sci. 98, 47–55.

Borges, A., 1944. Estação Pré-histórica de Mangulane. Boletim da Sociedade de Estudos da Colónia de Moçambique.

Brain, C., 2004. Swartkrans. A Cave's Chronicle of Early MAN. Transvaal Museum, Pretoria.

Bromage, T., Schrenk, F., Zonneveld, F., 1995. Paleoanthropology of the Malawi Rift: an early hominid mandible from the Chiwondo Beds, northern Malawi. J. Hum. Evol. 28, 71–108.

Betzler, C., Ring, U., 1995. Sedimentology of the Malawi Rift: facies and stratigraphy of the Chiwondo Beds, northern Malawi. J. Hum. Evol. 28, 23–35.

Brennan, B.J., Rink, W.J., McGuirl, E.L., Schwarcz, H.P., 1997. Beta doses in tooth enamel by 'one group' theory and the Rosy ESR dating software. Radiat. Meas. 27, 307–314.

Cheng, H., Edwards, R.L., Hoff, J., Gallup, C.D., Richards, D.A., Asmerom, Y., 2000. The half-lives of uranium-234 and thorium-230. Chem. Geol. 169, 17–33.

Clark, D., 1966. Initial investigation of the archeology of Karonga District. Malawi. Am. Anthropol. 68, 67–89.

Clark, D., 1988. The Middle Stone Age of East Africa and the beginnings of regional identity. J. World Prehist. 2, 235–305.

Clark, J.D., 2001. Kalambo Falls Prehistoric Site. The Earlier Cultures: Middle and Earlier Stone Age. Cambridge University Press, Cambridge.

Clark, D., Brown, K., 2001. The Twin Rivers Kopje, Zambia: stratigraphy, fauna, and artifact assemblages from the 1954 and 1956 excavations. J. Archaeol. Sci. 28, 305–330.

Clark, D., Haynes, V., 1970. An elephant butchery site at Mwanganda's village, Karonga, Malawi, and its relevance for Paleolithic Archaeology. World Archaeol. 1, 390–411.

Cohen, A., Stone, J., Beuning, K., Park, L., Reinthal, P., Dettman, D., Scholz, C., Johnson, T., King, J., Talbot, M., Brown, E., Ivory, S., 2007. Ecological consequences of early Late Pleistocene megadroughts in tropical Africa. Proc. Natl. Acad. Sci. U. S. A. 104, 16422–16427.

Dixey, F., 1927. The Tertiary and post-Tertiary lacustrine sediments of the Nyassan Rift-valley. Quart. J. Geol. Soc. Lond. 83, 432–437.

Fukuchi, T., 2001. Assessment of fault activity by ESR dating of fault gouge: an example of the 500 m core samples drilled into the Nojima earthquake fault in Japan. Quatern. Sci. Rev. 20, 1005–1008.

Goldberg, P., Sherwood, S., 2006. Deciphering human prehistory through the geoarchaeological study of cave sediments. Evol. Anthropol. 15, 20–36.

Gonder, M., Mortensen, H., Reed, F., de Sousa, A., Tishkoff, S., 2007. Whole-mtDNA genome sequence analysis of ancient African lineages. Mol. Biol. Evol. 24, 757–768.

Ikeya, M., 1975. Dating a stalactite by electron paramagnetic resonance. Nature 255, 48–50.

Johnson, T., Scholz, C., Talbot, M., Kelts, K., Dicketts, R., Ngobi, G., Beuning, K., Ssemmanda, I., McGill, J., 1996. Late Pleistocene desiccation of Lake Victoria and rapid evolution of Cichlid Fishes. Science 273, 1091–1093.

Juwayeyi, Y., Betzler, C., 1995. Archaeology of the Malawi Rift: the search continues for Early Stone Age occurrences in the Chiwondo Beds, northern Malawi. J. Hum. Evol. 28, 115–116.

Kingston, J., 2007. Shifting adaptive landscapes: progress and challenges in reconstructing early hominid environments. Yearb. Phys. Anthropol. 50, 20–58.

Kuman, K., Clarke, J., 2000. Stratigraphy, artefact industries, and hominid associations for Sterkfontein, member 5. J. Hum. Evol. 38, 827–847.

Lächelt, S., 2004. The Geology and Mineral Resources of Mozambique. Direcção Nacional de Geologia, Maputo.

Lahr, M., Foley, R., 1998. Towards a theory of modern human origins: geography, demography, and diversity in recent human evolution. Yearb. Phys. Anthropol. 41, 137–176.

Laville, H., Rigaud, J.P., Sackett, J., 1980. Rock Shelters of the Perigord: Geological Stratigraphy and Archaeological Succession. Academic Press, New York.

McCall, G., 2007. Behavioral ecological models of lithic technological change during the later Middle Stone Age of South Africa. J. Archaeol. Sci. 34, 1738–1751.

McKeague, A., 1976. Manual of Soil Sampling and Methods of Analysis. Soil Research Institute, Ottawa.

Manica, A., Amos, W., Balloux, F., Hanihara, T., 2007. The effect of ancient population bottlenecks on human phenotypic variation. Nature 448, 346–348.

Marean, C.W., Assefa, Z., 2005. The middle and Upper Pleistocene African record for the biological and behavioral origins of modern humans. In: Stahl, A. (Ed.), African Archaeology. Blackwell Publishing Ltd., Malden, pp. 93–129.

Marlowe, F., 2005. Hunter-gatherers and human evolution. Evol. Anthropol. 14, 54–67.

Mellars, P., 2006. Why did modern human populations disperse from Africa ca. 60,000 years ago? A new model. Proc. Natl. Acad. Sci. U. S. A. 103, 9381–9386.

Meneses, P., 1988. Idade da Pedra em Moçambique. Trabalhos de Arqueologia e Antropologia 5, 3–49.

Meneses, P., 1992. O mapa arqueológico de Moçambique (Idade da Pedra). Leba 7, 221–234.

Mercader, J., 2003. Foragers of the Congo: the early settlement of the Ituri forest. In: Mercader, J. (Ed.), Under the Canopy: The Archaeology of Tropical Rainforests. Rutgers University Press, pp. 93–116.

Mercader, J., Brooks, A., 2001. Across forests and savannas: later Stone Age assemblages from Ituri and Semliki, Northeast Democratic Republic of Congo. J. Anthropol. Res. 57, 197–217.

Mercader, J., Martí, R., 2003. The hunter-gatherer occupation of Atlantic Central Africa: new evidence from Equatorial Guinea Cameroon. In: Mercader, J. (Ed.), Under the Canopy: The Archaeology of Tropical Rainforests. Rutgers University Press, pp. 64–92.

Mercader, J., Martí, R., Martínez, J., Brooks, A., 2002. The nature of 'stone-lines' in the African quaternary record: archaeological resolution at the rainforest site of Mosumu, equatorial Guinea. Quat. Int. 89, 71–96.

Mercader, J., Bennett, T., Raja, M., 2008. Middle stone age starch aquisition in the Niassa Rift, Mozambique. Quaternary Research 70, 283–300.

Pickering, R., Hancox, P., Lee-Thorp, J., Grün, R., Mortimer, G., McCulloch, M., Berger, L., 2007. Stratigraphy, U-Th chronology, and paleoenvironment at Gladysvale Cave: insights into the climatic control of South African hominin-bearing cave deposits. J. Hum. Evol. 53, 602–619.

Ring, U., Betzler, C., 1995. Geology of the Malawi Rift: kinematic and tectonosedimentary background to the Chiwondo Beds, northern Malawi. J. Hum. Evol. 28, 7–21.

Rink, W.J., 1997. Electron spin resonance (ESR) dating and ESR applications in Quaternary science and archaeometry. Radiat. Meas. 27, 975–1025.

Scholz, C., Johnson, T., Cohen, A., King, J., Peck, J., Overpeck, J., Talbot, M., Brown, E., Kalindekafe, L., Amoako, P., Lyons, R., Shanahan, T., Castaneda, I., Heil, C., Forman, S., McHargue, L., Beuning, K., Gomez, J., Pierson, J., 2007. East African megadroughts between 135 and 75 thousand years ago and bearing on early-modern human origins. Proc. Natl. Acad. Sci. U. S. A. 104, 16416–16421.

Simões, M., 1951. A Préhistoria de Moçambique. Boletim da Sociedade de Estudos da Colónia de Moçambique 68, 115–152.

Simões, M., 1958. Sequência da Evolução da Indústria da Pedra em Moçambique a Sul do Save. Boletim da Sociedade de Estudos da Colónia de Moçambique 3, 149–156.

Sinclair, P., Morais, J., Adamowicz, L., Duarte, R., 1993. A perspective on archaeological research in Mozambique. In: Shaw, T., Sinclair, P., Andah, B., Okpoko, A. (Eds.), The Archaeology of Africa: Food, Metals, and Towns. Routledge, London, pp. 409–431.

Skinner, A.R., Blackwell, B., Chasteen, D., Shao, J., Min, S., 2000. Improvements in dating tooth enamel by ESR. Appl. Radiat. Isot. 52, 1337–1344.

Skinner, A.R., Rudolph, M.N., 1997. The use of the $E'$ signal in flint for ESR dating. Appl. Radiat. Isot. 47, 1399–1404.

Skinner, A.R., Blackwell, B., Martin, S., Blickstein, J., Golovanova, L., Doronichev, V., 2005. ESR dating at Mezmaiskaya Cave, Russia. Appl. Radiat. Isot. 62, 219–224.

Sperazza, M., Moore, J., Hendrix, S., 2004. High-resolution particle size analysis of naturally occurring very fine-grained sediment through laser diffractometry. J. Sediment. Res. 74, 736–743.

Woodward, J., Bailey, G., 2000. Sediments sources and terminal Pleistocene geomorphological processes recorded in rockshelter sequences in north-west Greece. In: Foster, I. (Ed.), Tracers in Geomorphology. John Wiley and Sons, New York, pp. 521–551.

Willoughby, P., 2001. Middle and Later Stone Age technology from the Lake Rukwa, Southwestern Tanzania. South African Archaeological Bulletin 56, 34–45.

Zhou, L.P., McDermott, F., Rhodes, E.J., Marseglia, E.A., Mellars, P.A., 1997. ESR and mass-spectrometric uranium-series dating of a mammoth tooth from Stanton Harcourt Oxfordshire, England. Quatern. Sci. Rev. 16, 727–738.